



MFI Zeolite Membranes and PV Separation of Isopropanol-Water Azeotropic Mixtures

A.A. Kittur^{1*}

¹Professor, Department of Chemistry, SDM College of Engineering and Technology, Dhavalgiri, Dharwad, India.

Mail ID: kittur1965@gmail.com¹

Orchid ID: 0000-0003-0845-1263*

Abstract

Membrane separation process has become one of the emerging technologies that undergo a rapid growth since few decades. Pervaporation (PV) is one among the membrane separation processes which gained foremost interest in the chemical and allied industries. It is an effective and energy-efficient technology that carries out separations, which are difficult to achieve by conventional separation processes. Inorganic membranes such as zeolite membranes with uniform, molecular-sized pores, selective adsorption and molecular sieving action offer unique type of pervaporation membrane for a number of separation processes. This paper presents the role of MFI-zeolite membrane and its progress in the pervaporation process. The fundamental aspects of pervaporation over different types of membranes are reviewed and compared. The focus of this paper is on zeolite membrane synthesis, membrane characterization and pervaporation studies. The transport mechanism during pervaporation is discussed and the issues related with pervaporation are addressed. Innovation and future development of zeolite membrane in pervaporation are also presented.

Keywords: Pervaporation, MFI zeolite, permeation, diffusion, Transport Mechanism

1. Introduction

Since few decades, membrane separation process has become one of the emerging technologies that underwent a rapid growth. It has drawn the keen interest of researchers in the separation technology area with its better performance compared to the conventional separation technology [1]. Membrane separation involves partially separating a feed containing a mixture of two or more components by using a semi-permeable barrier (membrane) through which one or more of the species moves faster than or other species. A membrane is a thin sheet of natural or synthetic material that covers a surface and is permeable to certain component in the solution. The main membrane separation technologies include microfiltration, ultrafiltration, reverse osmosis, nanofiltration, electrodialysis, gas-separation and pervaporation [2]. The principle of membrane separation process, type of membrane used, driving forces and examples of the application

of the established membrane separation technologies are discussed by various researchers. Most of the membrane separation technologies are well developed and established. Among these technologies, pervaporation is still a rapidly developing membrane separation technology [2]. Pervaporation (PV) is a process that has elements in common with reverse osmosis and membrane gas separation. It also has many similarities with vapor permeation, which uses gaseous components on the feed side of the membrane. However, the vapor permeation fluxes strongly depend on feed pressure whereas the pervaporation fluxes are independent of the feed pressures [3]. PV is used for the separation of azeotropic mixtures by partial vaporization through a porous membrane. The membrane acts as a selective barrier between the two phases, the liquid phase feed and the vapor phase permeate. It allows the desired components of the liquid feed to transfer



through it by vaporization [3]. Separation by pervaporation is almost independent of the vapor liquid equilibrium, because the transport resistance depends on the sorption equilibrium and mobility of the permeate components in the membrane. Vacuum is kept on the permeate side of the membrane while the atmospheric or elevated pressure is kept at the feed side of the membrane so that a pressure difference is created over the membrane in order to maintain the driving force for the pervaporation process. Figure 1 shows the overview of the pervaporation process. The desired component in the feed which is in the liquid form permeates through the membrane and evaporates while passing through the membrane because the partial pressure of the permeating component is kept lower than the equilibrium vapour pressure. PV is mild and effective for separation of those mixtures which cannot be subjected to the harsh conditions of distillation. It has advantages in terms of low energy consumption. It can be used for breaking azeotropes, dehydration of solvents and other volatile organics, organic/organic separations such as isopropanol-water mixture, xylene isomers separations, acid separations and wastewater purification [4,5]. Recently pervaporation has gained increasing interest on the part of the chemical industry as an effective and energy-efficient technology to carry out separations which were difficult to achieve by conventional means. This technology has better separation capacity and energy efficiency which could lead to 40–60% energy reductions. Different types of membranes are being used for pervaporation: polymeric membranes, ceramic membranes, and composite membranes. Over the last decades considerable efforts have been put in the development of ceramic membranes for pervaporation as these membranes show better resistance toward harsher chemical, pressure and thermal conditions. An example of the ceramic membranes is the zeolite membranes that have the unique properties of zeolite in a film-like configuration. Zeolite membranes have been widely used for pervaporation both laboratory studies and industrially [6,7]. In this paper, a critical assessment

of role of membrane in the pervaporation process is reported. The present study may lead to a better understanding of the fundamental aspects of separations by pervaporation through different types of membranes. Several methods used for the synthesis and characterization of inorganic ceramic membrane especially zeolite membrane are presented. The theory for the transport mechanism in pervaporation which is essential not only for a better understanding of the process itself but also for design purposes is also reviewed. Current and potential applications of pervaporation through zeolite membrane are discussed. Moreover, common problems encountered and issues related with pervaporation are addressed. Finally, an outlook of the innovation and future development of zeolite membrane in pervaporation is presented.

2. Experimental Methods

2.1 Materials

Isopropanol and hydrochloric acid were purchased from s. d. fine Chemicals Ltd., Mumbai, India. Tetraethylorthosilicate (TEOS) and TPAOS were procured from E. Merck (India) Ltd., Mumbai. All the chemicals are of reagent grade and were used without further purification. Double distilled water was used throughout the study.

2.2 Zeolite membrane synthesis

Zeolite membranes that are synthesized so far have shown good separation performance, but the permeance is too low for practical application [8]. One of the challenges for the preparation of zeolite membrane is to prepare zeolite membrane with high permeance and high separation selectivity. In order to obtain a better separation performance, zeolite membrane should be preferably made of pure zeolite crystals with uniform and small particle size. **Hydrothermal Synthesis of MFI zeolite membrane:** A hydrothermal treatment implies the use of an aqueous solution, synthesis gel, which is heated in an autoclave at a certain temperature under autogenous pressure. The chemicals in the synthesis gel include the silicon and aluminum sources in the presence of a mineralizing agent commonly sodium hydroxide or alternatively fluoride ion and in some cases a structure-directing agent (SDA). Most

zeolite film syntheses are carried out using the static hydrothermal method. In this process the nutrition are consumed quickly at the interface of the zeolite film and the synthesis solution, which results in a large concentration gradient in the bulk solution and this might change the solution's composition. The high concentration and large thermal gradients might result in defect full membranes which intern affect film performance significantly. Some new methods have been investigated under dynamic environments to avoid or reduce the negative influences mentioned above [9-15]. A new dynamic synthesis apparatus to produce a b-oriented MFI zeolite film in which the synthesis conditions were dynamic because of the rotation of autoclave. Pure silica MFI (silicalite-1) films on stainless steel substrates were prepared as follows: Mirror stainless steel 202 plates (20 mm × 20 mm) were immersed in a hydrogen peroxide solution for 45 min and then rinsed with deionized water after which it was dried at 60 °C before the synthesis of the zeolite films. A

synthesis solution with a molar composition of 1TEOS:0.32TPAOH:165H₂O was made by slowly adding tetraethylorthosilicate to a solution of tetrapropylammonium hydroxide (TPAOH and water while stirring. A clear synthesis solution was obtained after stirring at room temperature for 4 h. The synthesis solution (90 g) was loaded directly without filtering into a Teflon-lined stainless steel autoclave (110 ml). Figure 1 shows the experimental apparatus used in this work to synthesize the zeolite films. A metal substrate was placed vertically in a Teflon holder at the middle of the autoclave and immersed into the synthesis solution. The autoclave was then sealed and heated in a rotating convection oven at a specific temperature and held there for a certain amount of time. In the rotating convection oven the autoclaves were fixed in a stationary barrier, which could rotate with the axis. After the synthesis the mixture was quenched. The samples were recovered, thoroughly washed with deionized water, and dried at 60 °C.

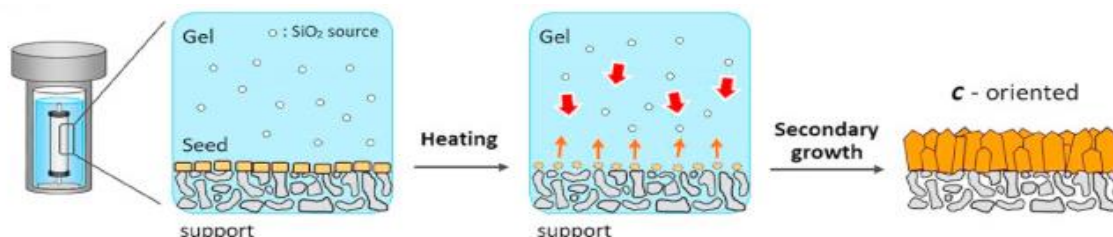


Figure 1 Hydrothermal Synthesis of MFI Zeolites

The MFI topological structure first consists of five-membered rings composed of [TO₄] tetrahedra (the central atom T is generally Si, Al, Ti, Ga, or Fe), then the primary structural units composed of eight five-membered rings form a pentasil chain structure through common edge connections. Finally, the pentasil chain is assembled into an anisotropic three-dimensional pore channel by sharing the vertex oxygen atoms [16]. MFI zeolite membranes can be subdivided into S-1, ZSM-5, and TS-1 membranes based on the constituent elements [1]. S-1 is an all silica zeolite membrane because of its good hydrophobicity and regular pore size, which is approximately consistent with the molecular size, so it is widely used in gas-gas (e.g., isomers of p-

xylene) and liquid-liquid (e.g., mixture of ethanol and water) separation processes.

It is well known that in the structure of MFI zeolite membranes, the sinusoidal channel (0.51 × 0.55 nm, approximately circular section) parallel to the a-axis and the straight channel (0.53 × 0.56 nm, approximately elliptical cross section) parallel to the b-axis are connected [17], and a tortuous path exists along the c-axis direction as shown in Figure 1. A previous study [18] has shown that when tetrapropylammonium hydroxide (TPAOH) is used as a structure-directing agent (SDA), the MFI grains have a characteristic coffin shape and the three-dimensional size is consistently longer along the c-axis and smaller along the b-axis ($L_c > L_a > L_b$).

Therefore, the mass transfer paths and efficiencies of MFI zeolite membranes with different orientations are greatly different owing to the influence of grain size, channel shape, and tortuosity. At present, a-, b-, c-, and (*hOh*)-oriented zeolite membranes have been synthesized through proper regulation and control. However, both experimental data and simulation results show that the diffusion coefficient along the straight channel is approximately three times that on the channel perpendicular to this direction. Compared with the membranes of other orientations, the synthesis of b-oriented MFI zeolite membranes to shorten the mass transfer path and enhance the diffusion efficiency has greatly attracted the interests of researchers [1].

2.3 Membrane characterization

Membrane characterization is essential in order to

evaluate the quality of the synthesized membrane. The morphology of the silicalite films synthesized was examined by scanning electron microscopy (SEM) at 8 kV using a Hitachi S-4800 microscope. X-ray diffraction (XRD) patterns were collected on an analytical X' PertPro diffractometer using Cu K α radiation.

2.4 Pervaporation experiments

PV experiments were performed using an indigenously designed apparatus as shown in Figure 2. The effective surface area of the membrane in contact with the feed mixture is 34.23 cm² and the capacity of the feed compartment is about 250 cm³. The vacuum in the downstream side of the apparatus was maintained (10 Torr) using a two-stage vacuum pump (Toshniwal, Chennai, India).

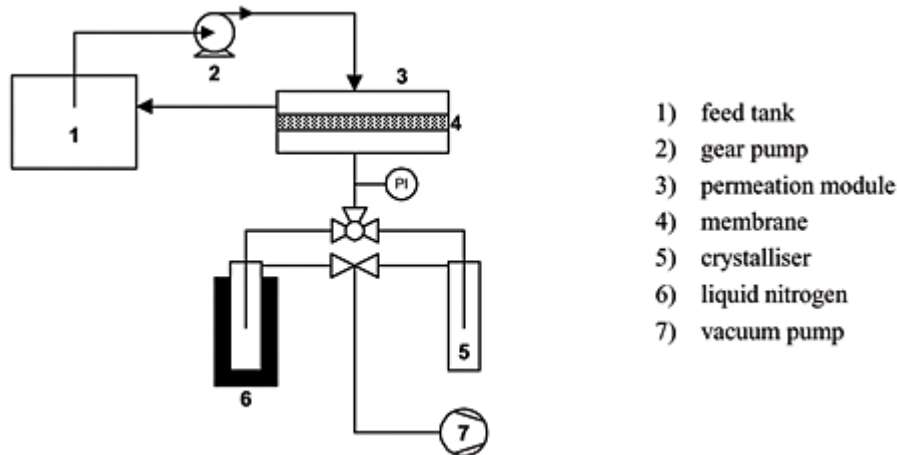


Figure 2 Experimental Setup of Pervaporation

The water composition in the feed mixture was varied from 10 to 50 mass %. The test membrane was allowed to equilibrate for about 2 hours in the feed compartment before performing the PV experiment with a known volume of feed mixture. After an equilibrium was attained, the permeate was collected in traps immersed in the liquid nitrogen on the downstream side at timed intervals and experiments were carried out at 30°C. The flux was calculated by weighing the permeate on a digital microbalance (Mettler B204-S, Toledo, Switzerland) with an accuracy of ± 0.01 mg. The

compositions of water and isopropanol were estimated by measuring the refractive index of the permeate within an accuracy of ± 0.0001 units using Abbe's Refractometer (Atago-3T, Japan) and using standard graph of refractive index vs known compositions of water-isopropanol mixture. The results from the permeation of water-isopropanol mixtures during the pervaporation were reproducible, and the errors inherent in the pervaporation measurements were in the order of a few percent. From the PV data, separation performances of the membranes can be assessed in

terms of total flux (J), separation selectivity (α_{sep}) and pervaporation separation index (PSI) and these were calculated, respectively, using the following equations:

$$J = \frac{W}{A \cdot t} \quad (2)$$

$$\alpha_{sep} = \frac{P_w / P_{IPA}}{F_w / F_{IPA}} \quad (3)$$

$$PSI = J (\alpha_{sep} - 1) \quad (4)$$

Here, W is the mass of permeate (kg); A , the area of the membrane in contact with the feed mixture (m^2); t , the permeation time (h); P_w and $P_{dioxane}$ are the mass fractions of water and dioxane in the permeate, respectively. F_w and $F_{dioxane}$ are the respective mass fractions of water and dioxane in the feed.

3. Results and Discussion

3.1 X-ray diffraction studies

To confirm the orientation of the zeolite films XRD was carried out, as shown in Figure 3. Apart from the peak at $2\theta = 43.46^\circ$ that corresponds to the stainless steel substrate, five sharp peaks were observed at $2\theta = 8.87^\circ, 17.77^\circ, 26.80^\circ, 35.99^\circ,$ and 45.45° and these are attributed to the (020), (040), (060), (080), and (0100) orientations of the MFI zeolite crystals [19], respectively.

The MFI zeolite films synthesized in our work are predominantly b-oriented. However, the two small peaks at $2\theta = 35.75^\circ$ and 45.15° , as shown in Figure 3, are assigned to the (800) and (1000) orientations in the MFI zeolite crystals [20], respectively. The two small peaks indicate that some a-oriented MFI crystals were present in the film synthesized using the static method. The amplified drawings show three small peaks that are attributed to the (200), (400) and (600) orientations and these are distinguished with difficulty because of the small peak areas, the overlapping (0k0) peaks and the small difference in 2θ between (h00) and (0k0). Compared with Figure 3, the two peaks attributed to the (800) and (1000) orientations in the MFI zeolite crystals were smaller, as shown in Figure 3, which

indicates that less a-oriented MFI crystals are present in the film synthesized using the dynamic method.

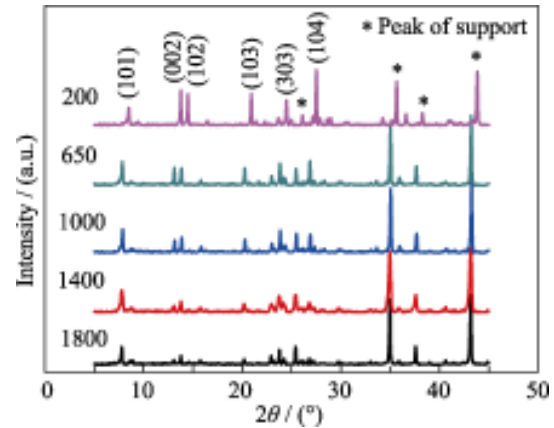


Figure 3 WXR Analysis of MFI Zeolite Membranes

3.2 SEM Study

A continuous MFI zeolite membrane was formed on the surface of the $\alpha\text{-Al}_2\text{O}_3$ support through the dynamic growth method. Figure 3 presents the top and cross-sectional view of the MFI zeolite membrane with and without a template. From the top-view images, it can be seen that both membranes are continuing without any obvious defect on the surface, and the MFI membrane prepared by the template-free method shows relatively larger crystal size and better inter-growth with much higher integrity when compared with that from the template method. As to their cross-sectional analysis, both of the zeolite layer and Al_2O_3 support layer can be clearly distinguished in the images. Although they are synthesized under different hydrothermal conditions, the two membranes have similar thicknesses, $30\ \mu\text{m}$ and $10\ \mu\text{m}$ for the templated method and for the template-free method. Besides, the zeolite crystal boundary of the membrane fabricated with the templated method is much clearer than that from the template-free method. This may be caused by the shrinkage of the lattice parameters during the template elimination process. It should be noted that the resulting shrinkage of the crystal size may generate some non-zeolite micropores within the membrane structure, which will inevitably affect the selectivity during the pervaporation process.

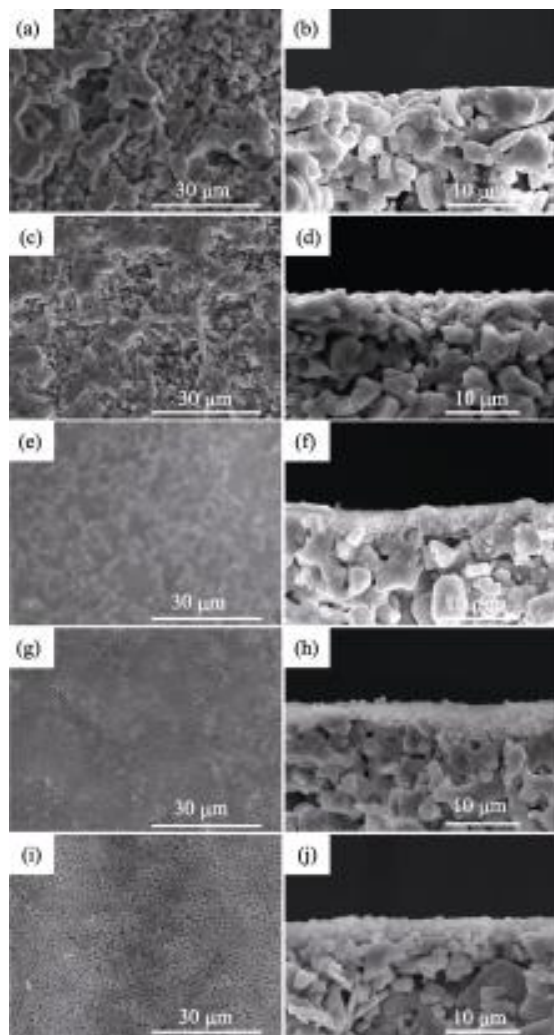


Figure 4 SEM Pictures of MFI Zeolite Membranes prepared with Different-Size Seeds in $H_2O/SiO_2=1000$ Synthetic Solution

The XRD data (Figure 3) and the SEM images (Figure 4) of the films synthesized using the two methods indicate that a better orientation is obtained by dynamic hydrothermal synthesis. Since the synthesis conditions differed greatly between the static and dynamic hydrothermal methods the size distribution of the zeolite crystals might be different.

3.3 Transport mechanism during pervaporation

In a pervaporation process, transport through the membrane is generally described by a so-called 'solution-diffusion mechanism' [21] which consist of three successive steps:

- Selective sorption of the species in the liquid mixture at the feed/membrane interface
- Diffusion through the membrane due to concentration gradient
- Desorption at the membrane/permeate interface into the vapor phase permeate side

3.4 Pervaporation studies

A typical experimental set-up for pervaporation studies is shown in Figure 2. The feed is placed in the feed tank, heated and re-circulated. A vacuum is applied on the downstream side and permeate pressure is maintained below 10 torr for most laboratory-scale studies.

Effect of seed size on pervaporation properties:

Figure 5 shows the effect of seed size on the total permeation flux for all the membranes at 30°C. It is observed that the total permeation flux increased almost linearly for all the zeolite membranes with increasing the amount of water in the feed. This is due to an increase of selective interaction between water molecules and hydroxyl groups of zeolite membranes. This interaction becomes more predominant at higher concentration of water, since water causes a greater degree of interaction than that of isopropanol with these membranes. On the contrary, the permeation flux slightly increased from membrane M-1 to M-5 with increasing the seed size as can be seen in Figure. This is because of significant reduction of free-volume in the membrane matrix. The results obtained are tabulated in the Table 1.

The overall selectivity of a membrane in PV process is generally determined on the basis of interaction between the membrane and permeating molecules, molecular size of the permeating species and pore diameter of the membrane. It is observed that the selectivity increased linearly from membrane M-1 to M-5 upon increasing the seed size as seen from Figure 5. This is due to a reduction of free-volume in membrane matrix and decreased hydrophilic character of the membranes, which together responsible for the increased selective interaction between membrane and the water molecules.

Table 1 Pervaporation Performance of MFI Zeolite Membranes prepared with Seeds of Different Size

No.	Seed size/ μm	H ₂ O/ SiO ₂	Time/h	$J/ (\text{kg}\cdot\text{m}^{-2}\cdot\text{h}^{-1})$	α	psI
M1	0.4	1000	24	4.09	47	192.23
M2	0.8	1000	24	4.22	39	164.58
M3	1.3	1000	24	4.30	35	150.05
M4	1.6	1000	24	4.52	30	135.6
M5	2.0	1000	24	5.10	24	122.4

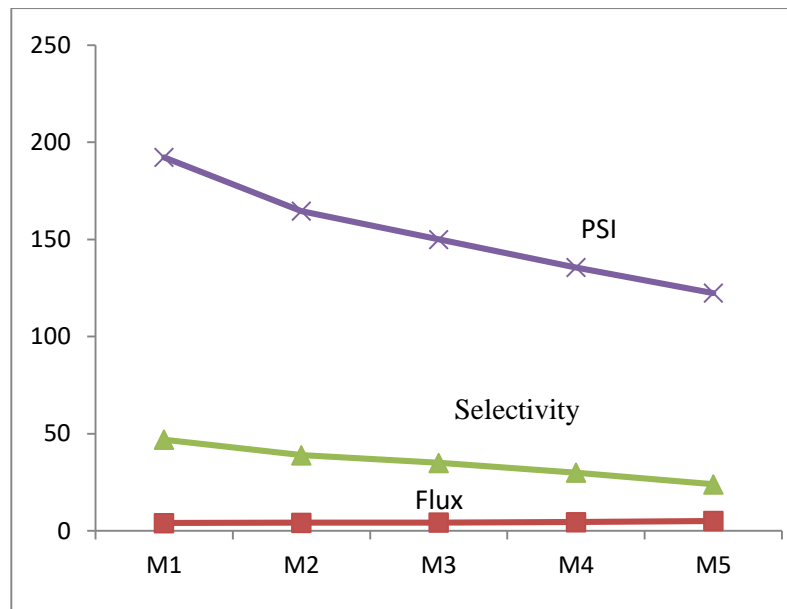


Figure 5 Effect of Seed Size on Flux, Separation Factor and PSI

Pervaporation separation index (PSI):

Pervaporation separation index (PSI), which is a relative measure of the separation ability of a membrane, has been defined as the product of total permeation and separation factor. This index can be used as a relative guideline index for the design of pervaporation membrane separation processes and also to select a membrane with an optimal combination of flux and selectivity. Figure 5 shows the variation of *PSI* as a function of seed size variation in the membranes for 10 mass % of water

in the feed at 30°C. It is found that *PSI* values increased from M-1 to M-5. This signifies that the membranes of the present study showed better performances at higher seed size.

Conclusion

Pervaporation has advantages in separating azeotropes, close-boiling point mixtures and thermally sensitive compounds. This technology will be more economical compared to conventional separation processes, such as distillation or adsorption since it is more energy efficient than



distillation. In addition, it is more environmental friendly because unlike in distillation, no third component is added. On the other hand, zeolite membrane has additional advantages in separating azeotropic mixtures. Zeolite membranes with variation in seed size showed a significant performance while separating water-isopropanol mixtures. The performance of these membranes was explained on the basis of a reduction of free-volume and decreased hydrophilic character. The membrane having high seed size showed the low separation selectivity of 24 with a flux of 5.1×10^{-1} kg/m² h at 30°C for 10 mass % of water in the feed. The PV separation index data also support that membrane with a higher seed size showed an excellent PV performance.

References

- [1]. Yichuan Li, Guofu Zhu, Yu Wang, Yongming Chai, Chenguang Liu *Microporous and Mesoporous Materials* 312 (2021) 110790.
- [2]. P. Shao, R.Y.M. Haung *Journal of Membrane Science*, 287 (2007) 162-179.
- [3]. Lijun Shan, Jia Shao, Zhengbao Wang, Yushan Yan *Journal of Membrane Science* (2004) 319-329.
- [4]. Shin-Ling Wee, Ching-Thian Tye, Subhash Bhatia, 63 (2008) 500-516.
- [5]. Sekulic et al. / *Journal of Membrane Science* 254 (2005) 267-274.
- [6]. F. T. de Bruijn, L. Sun, Z. Olujic, P. J. Jansens and F. Kapteijn, *J. Membr. Sci.*, 223 (2003) 141-156.
- [7]. Vasudevan V. Namboodiri, Leland M. Vane, *Journal of Membrane Science*, Volume 306, Issues 1-2, 1 December 2007, Pages 209-215.
- [8]. M.L. Gimenes L. Liu, X. Feng, *Journal of Membrane Science* Volume 295, 2007, 71-79.
- [9]. E. E. Mcleary, J. C. Jansen, and F. Kapteijn, *Microporous Mesoporous Mater.* 90, 198 (2006).
- [10]. Aguado S, Gascon J, Jansen J C, Kapteijn F. *Microporous Mesoporous Mater.*, 2009, 120: 170-19.
- [11]. Khajavi S, Kapteijn F, Jansen J C. *J Membr Sci*, 2007, 299: 63-20.
- [12]. Pera-Titus M, Mallada R, Llorens J, Cunill F, Santamaria J. *J Membr Sci*, 2006, 278: 401-21.
- [13]. Xu H H, Shah D B, Talu O. *Zeolites*, 1997, 19: 114-22.
- [14]. Yamazaki S, Tsutsumi K. *Microporous Mesoporous Mater.*, 2000, 37: 67-23.
- [15]. Tiscareño-Lechuga F, Tellez C, Menendez M, Santamaria J. *J Membr Sci*, 2003, 212: 135-24.
- [16]. Huang A S, Yang W S, Liu J. *Sep Purif Technol*, 2007, 56: 158.
- [17]. Karakiliç, Pelin; Toyoda, Ryo; Kapteijn, Freek; Nijmeijer, Arian; Winnubst, Louis, DOI 10.1016/j.micromeso.2018.09.020.
- [18]. Aguado, S., Gascón, J., Jansen, J. C., & Kapteijn, F. (2009). Continuous synthesis of NaA zeolite membranes. *Microporous and Mesoporous Materials*, 120(1-2), 170-176. <https://doi.org/10.1016/j.micromeso.2008.08.062>.
- [19]. X. Su, S. T. Xu, P. Tian ... *Chinese Journal of Catalysis* 37 (2016) 340-348.
- [20]. H. Pan¹, Z. Liang¹, L. Hua-Zheng¹, L. Hong-Jian¹, Y. Jian-hua², W. Jin-Qu¹, *Journal of Inorganic Materials* » 2018, Vol. 33 » Issue (3): 345-351.